An Investigation into the Primary and Subharmonic Resonances of the Swing Equation

ANASTASIA SOFRONIOU, BHAIRAVI PREMNATH
School of Computing and Engineering, University of West London,
St. Mary's Road, W5 5RF, UNITED KINGDOM

Abstract: A study is conducted to obtain a deeper insight into the primary and subharmonic resonances of the swing equation. The primary resonance, which can result in increased oscillatory responses, voltage instability, and potential system collapse, happens when the external disturbance frequency coincides with the natural frequency of the system. Subharmonic resonance occurs when the disturbance frequency is an integer fraction of the natural frequency, leading to low-frequency oscillations and possible equipment damage. The purpose of this study is to provide an extension of the existing literature of the effects of primary resonance and further provide a thorough understanding of subharmonic resonance on the stability of a certain power system paradigm. Motivated by the rich nonlinear dynamical behaviour exhibited by this evergreen model, analytical and numerical techniques are employed to examine the underlying principles, creating an efficient control solution for this resonant-related problem. The main objective of this research is to provide a comprehensive understanding of the primary and subharmonic resonances considering the dynamical and bifurcational behaviour of the underlying swing equation, whereby both analytical and numerical techniques are employed, allowing for an identification of certain precursors to chaos that may lead and cater for the safe operation of practical problems.

Key-Words: nonlinear dynamics, swing equation, resonance

Received: October 21, 2022. Revised: May 16, 2023. Accepted: July 15, 2023. Published: August 11, 2023.

1 Introduction

The swing equation can be considered as a foundational model for analysing the dynamic behaviour of power systems, particularly the oscillatory motion of synchronous generators. To preserve the stability and dependability of power infrastructures, it is necessary to comprehend the resonance phenomena that can occur in this nonlinear system. Primary resonance and subharmonic resonance are two significant resonance types undergone in the swing equation. This paper is an expansion of prior work, [1] and builds on its conclusions in order to explain the subharmonic resonance.

Primary and subharmonic resonances play a crucial role in determining the stability of dynamical system. The idea of disturbances, which are abrupt changes to the system's operating quantities, is strongly related to the concept of stability in a power system. A minor perturbation can nonetheless have a fascinating and varied impact on a system's dynamics, [1]. The dynamical behaviour of this system is observed through altering the variables in the equation whilst keeping other factors constant. The primary resonance is considered to be important when studying the swing equation. Under primary resonance conditions, a small-amplitude excitation may result in a relatively large-amplitude response if the forcing frequency is close to the linearised natural frequency, [2]. Additionally, nonlinear dynamic behaviours such as saddle-node bifurcations could be present in the steady-state forced response of the nonlinear system, [3].

Primary resonance is when the excitation frequency is approximately close to the natural frequency of the system. The subharmonic resonance on the other hand, is when the excitation frequency is a multiple of the natural frequency, [4]. Numerous studies have been conducted in order to examine these resonances in nonlinear power systems, to comprehend the underlying principles, and to create efficient control schemes. For instance, to investigate the effect of primary and subharmonic resonance on the stability of power systems, researchers have used mathematical modelling, simulation studies, and experimental validations. To reduce the negative impacts of resonance and improve system stability, these studies have helped to develop cutting-edge control techniques such as adaptive control, robust control, and damping controllers.

1.1 Brief Literature Review

A vital component of guaranteeing the dependable and effective operation of electric circuits is the stability of power systems, [5]. When a power system is stable, it can continue to operate within reasonable bounds and retain its balance in the face of perturbations. The swing equation is crucial to understanding the dynamic behaviour of power systems among other stability issues, [6]. Resonance at the primary and subharmonic levels is another important element that might impact system stability. Transient stability and steady-state stability are the two main subtypes of power system stability. The capacity of the system to return to a stable operating point following a significant disruption, such as a fault or a sudden loss load, is referred to as transient stability, [7]. The ability of the system to remain stable in the face of little disruptions, such as slight changes in power demand or generation, is the subject of steady-state stability, also known as small-signal stability, [8].

A key dynamic equation used to simulate the behaviour of synchronous generators in a power system is the swing equation. It describes the speed dynamics and rotor angle stability of synchronous machines under transient situations. The swing equation is predicated on the idea that a generator's electrical output is inversely proportional to the angle between its rotor and the system's voltage at its terminal, [9].

Primary resonance happens when the natural frequency of a power system coincides with the frequency of an applied external disturbance. It is an occurrence that could result in unstable oscillations and bring about system instability, [10]. Primary resonance is frequently linked to low-frequency electromechanical modes of oscillation, which are frequently exemplified by the interaction between generators and their corresponding control systems, [11]. It can cause significant oscillations in generator rotor angles, which, if left unchecked, might eventually cause cascading failures and blackouts, [12]. Subharmonic resonance is a phenomenon where a power system's response shows oscillations at frequencies lower than the applied external disturbance's frequency, [13]. It happens when a power system's inherent frequency falls below the disturbance frequency. Power electronic components, such as voltage source converters or thyristor-controlled reactors, can interact with the power system to cause subharmonic resonance, [14]. If not reduced, it may result in long-lasting oscillations and instability. Power electronic equipment that is connected to the grid must be designed and operated in a way that takes subharmonic resonance into account, [15].

A comparative analysis of primary and subharmonic resonance is essential for comprehending their distinctive characteristics and implications for the stability of a power system. The authors in [16], used both analytical and experimental techniques, to carry out a comparison between the two resonance phenomena. Their research illuminated the similarities and distinctions between primary and subharmonic resonance, highlighting the significance of a thorough analysis, [16]. The development of classification techniques has enabled improved identification and differentiation of primary and subharmonic resonance. It has been demonstrated that machine learning algorithms, such as neural networks and support vector machines, can accurately classify resonance varieties. The authors in [17], presented a neural network-based method for the classification of resonance phenomena in real time, allowing for rapid response to critical stability events. The authors in [18], not only examined the effect of control strategies on subharmonic resonance, but also emphasised the significance of considering system parameter variations when evaluating the dynamic behaviour of primary and subharmonic resonances.

For electrical circuits and grids to operate reliably and efficiently, power system stability plays a key role. When examining the dynamic behaviour of power systems, particularly when examining rotor angle stability and speed dynamics, the swing equation is crucial. Resonance on the primary and subharmonic scales is a major phenomenon that can impact the stability of a power system, [19]. Subharmonic resonance involves oscillations at frequencies lower than the disturbance frequency, whereas primary resonance happens when the system's intrinsic frequency coincides with the frequency of an applied external disturbance hence it is vital when studying about a system's stability, [20]. Effective stability analysis, regulation, and mitigation measures in power systems depend on a thorough understanding of these phenomena. To ensure the stability and resilience of electricity systems in the face of changing grid circumstances and difficulties, more study and breakthroughs in these fields are essential.

Basins of attraction are regions in the state space where the trajectories of the system converge to particular attractors. Studies have examined the basins of attraction relating to primary and subharmonic resonance in power systems. Various techniques, including bifurcation

analysis, numerical simulations, and Lyapunov exponent calculations, have been utilised in these studies to determine the boundaries and characteristics of the basins of attraction, [21] which will also be employed here within. To obtain insight into the stability boundaries and robustness of power systems, researchers have investigated the effects of system parameters, initial conditions, and control strategies on systems.

2 Methodology

2.1 Analytical Work

The swing equation was derived from the Law of Rotation, which is fundamental in characterising the motion of rotating bodies and is based on Newtonian mechanics. Synchronous generators exhibit rotational behaviour when connected to the electrical grid in the context of power systems. By applying Newton's second law of motion to the synchronous generator while taking into account the mechanical and electrical torques acting on the rotor and by also considering the inertia of the rotating mass and the damping effects, the equation governing the dynamic motion of the generator rotor can be derived, [1], [6]. The swing equation is a nonlinear differential equation of the second order that represents the angle deviation of a generator's rotor from its synchronous position as a function of time.

The damping term of the swing equation that characterises the motion of the rotor of the machine used in this investigation is as follows, [6]:

$$\frac{2H}{\omega_R}\frac{d^2\theta}{dt^2} + D\frac{d\theta}{dt} = P_m - \frac{V_G V_B}{X_G}\sin(\theta - \theta_B) \quad (1)$$

$$V_{\mathrm{B}} = V_{B0} + V_{\mathrm{B1}}\cos(\Omega t + \phi_v) \quad (2)$$

$$\theta_B = \theta_{B0} + \theta_{B1}\cos(\Omega t + \phi_0) \quad (3)$$

with
$\omega_R = Constant\ angular\ velocity$,
H= Inertia,
D= Damping,
$\mathrm{P}_m = Mechanical\ Power$,
$\mathrm{V}_G = Voltage\ of\ machine$,
$\mathrm{X}_G = Transient\ Reactance$,
$\mathrm{V}_B = Voltage\ of\ bus$,
$\theta_B = phase\ of\ bus$.

V_{B1} *and* θ_{B1} *magnitudes assumed to be small.*

To achieve a deeper comprehension of the phenomenon of subharmonic resonance, it is necessary to conduct a thorough mathematical analysis of the swing equation. Various mathematical techniques, including algebraic methods, Taylor expansion, and substitution, are employed to achieve this objective. The objective is to develop a final equation for use in perturbation analysis, with a particular emphasis on understanding subharmonic resonance in the swing equation. Algebraic techniques such as simplifying complex expressions, factoring, combining like elements, and rearranging the equation are adopted to make further analysis easier. Using Taylor expansion, reduces the complexity of certain nonlinear terms in the swing equation, making it simpler to manipulate and analyse.

Allowing consideration for the transformations,

$$\theta - \theta_B = \delta_0 + \eta \quad (4)$$

$$\delta_0 = \theta_0 - \theta_{B0} \quad (5)$$

$$\eta = \Delta\theta - \theta_{B1}\cos(\omega t + \phi_0) \quad (6)$$

After manipulating equation (1), the following is obtained which is used for further analysis with regard to primary and subharmonic resonances:

$$\frac{d^2\eta}{dt^2} + \frac{\omega_R D}{2H}\frac{d\eta}{dt} + K\eta = \alpha_2\eta^2 + \alpha_3\eta^3 + \mathrm{G}_1\eta\cos(\Omega t + \phi_v) + G_2\eta^2\cos(\Omega t + \phi_v) + G_3\eta^3\cos(\Omega t + \phi_v) + Q\cos(\Omega t + \phi_e). \quad (7)$$

Primary Resonance

The primary resonance is observed when the natural frequency is approximately equal to the excitation frequency of the system. The perturbation analysis for this case has been carried out previously by the authors, [1], thus this paper initially provides an extension to that work by considering the basins of attraction of the swing equation under a variation of the parameters V_{B1} and θ_{B1}. The notation employed here within is consistent to, [1].

Perturbation Analysis for Subharmonic resonance

This method uses multiple scales to determine second order approximate expression for period-two solutions for the case $\Omega \simeq 2\omega_0$.

This solution can be used to predict the onset of the complex dynamics and stability. Hence the solution becomes less accurate as excitation amplitude increases because of its inability to account for frequency shift due to the external excitation. Introducing a small dimensionless parameter ε, which is used as a bookkeeping device.

Let

$$\eta = O(\varepsilon) \quad then \quad \frac{\omega_R D}{2H} = O(\varepsilon)$$

$$G_1 = O(\varepsilon) \quad Q = O(\varepsilon)$$

and

$$V_{B1} = O(\varepsilon) \; and \; \theta_{B1} = 0(\varepsilon)$$

Then the final equation from swing equation derivation above has the following coefficients,

$$G_1 = \varepsilon g_1$$

$$G_2 = \varepsilon g_2$$

$$G_3 = \varepsilon g_3$$

$$Q = \varepsilon q$$

After some mathematical operations equation (7) is formulated as follows,

$$\ddot{\eta} + 2\varepsilon\mu\dot{\eta} + \omega_0^2\eta = \alpha_2\eta^2 + \alpha_3\eta^3 + \varepsilon g_1\eta cos(\Omega t + \phi_v) + \varepsilon g_2\eta^2\cos(\Omega t + \phi_v) + \varepsilon g_3\eta^3\cos(\Omega t + \phi_v) + \varepsilon q\cos(\Omega t + \phi_e)$$

where $\mu = \frac{\omega_R D}{4H}$.

The solution to this above equation should be in the form of,

$$\eta(t;\varepsilon) = \varepsilon\eta_1(T_0, T_1, T_2) + \varepsilon^2\eta_2(T_0, T_1, T_2) + \varepsilon^3\eta_3(T_0, T_1, T_2) + ... \quad (8)$$

First derivative of this equation will be,

$$\frac{d}{dt} = D_0 + \varepsilon D_1 + \varepsilon^2 D_2 + ... \quad (9)$$

Second derivative of the equation is,

$$\frac{d^2}{dt^2} = D_O^2 + 2\varepsilon D_0 D_1 + \varepsilon^2(2D_0 D_2 + D_1^2) + ... \quad (10)$$

where

$$D_n = \frac{\partial}{\partial T_n}.$$

Also considering the equation where σ is introduced as a detuning parameter:

$$\omega_0^2 = \frac{1}{4}\Omega^2 + \varepsilon\sigma \quad (11)$$

and substituting equations (8), (9), (10) and (11) into (7) gives

$$\ddot{\eta} + 2\varepsilon\mu\dot{\eta} + (\frac{1}{4}\Omega^2 + \varepsilon\sigma)[\varepsilon\eta_1(T_0, T_1, T_2) + \varepsilon^2\eta_2(T_0, T_1, T_2) + \varepsilon^3\eta_3(T_0, T_1, T_2) + ...] = \alpha_2(\varepsilon^2\eta_1^2 + \varepsilon^4\eta_2^2 + \varepsilon^6\eta_3^2 + ...) + \alpha_3(\varepsilon^3\eta_1^3 + \varepsilon^6\eta_2^3 + \varepsilon^9\eta_3^3 + ...) + \varepsilon g_1(\varepsilon\eta_1 + \varepsilon^2\eta_2 + \varepsilon^3\eta_3)\cos(\Omega t + \phi_v) + \varepsilon g_2(\varepsilon^2\eta_1^2 + \varepsilon^4\eta_1^2 + \varepsilon^6\eta_3^2)\cos(\Omega t + \phi_v) + \varepsilon g_3(\varepsilon^3\eta_1^3 + \varepsilon^6\eta_2^3 + \varepsilon^9\eta_3^3 + ...) + \varepsilon q\cos(\Omega t + \phi_e)$$

Equating coefficients of like powers of ε,

$$\varepsilon/: \; \eta_1 D_0^2 + \frac{1}{4}\eta_1\Omega^2 = qcos(\Omega t + \phi_e) \quad (12)$$

$$\varepsilon^2/: \; \eta_2 D_0^2 + \frac{1}{4}\eta_2\Omega^2 + 2D_0 D_1\eta_1 + \sigma\eta_1 = \alpha_2\eta_1^2 + g_1\eta_1 cos(\Omega T_0 + \phi_v) \quad (13)$$

$$\varepsilon^3/: \; D_0^2\eta_3 + 2D_0 D_1\eta_2 + (D_1^2 + 2D_0 D_2)\eta_1 + 2\mu D_0\eta_1 + \tfrac{1}{4}\Omega^2\eta_3 + \sigma\eta_2 = 2\alpha_2\eta_1\eta_2 + \alpha_3\eta_1^3 + g_1\eta_2 cos(\Omega T_0 + \phi_v) + g_2\eta_1^2 cos(\Omega T_0 + \phi_v) \quad (14)$$

Solution to equation (12) can be in two forms,

$$(i) \; \eta_1 = a(T_0, T_1, T_2)\, cos\,[\frac{1}{2}\Omega T_0 + \beta(T_0, T_1, T_2)] + 2\Lambda cos(\Omega T_0 + \phi_e). \quad (15)$$

$$(ii) \; \eta_1 = A(T_1, T_2)e^{\frac{1}{2}i\Omega T_0} + \bar{A}(T_1, T_2)e^{\frac{-1}{2}i\Omega T_0} + \Lambda e^{i\Omega T_0} + \bar{\Lambda}e^{-i\Omega T_0} \quad (16)$$

It is given that

$$N = \frac{-2q}{3\Omega^2} e^{i\phi_e} \qquad (17a)$$

Comparing coefficients in equations (15) and (16) gives:

$$A = \frac{1}{2} a e^{i\beta} \qquad (17b)$$

Substituting equation (16) in (13) gives the following,

$$D_0^2\eta_2 + \frac{1}{4}\Omega^2\eta_2 = -2\mu D_0(Ae^{\frac{1}{2}i\Omega T_0} + \bar{A}e^{\frac{-1}{2}i\Omega T_0} + \mathrm{N}e^{i\Omega T_0} + \bar{N}e^{-i\Omega T_0}) - 2D_0D_1(Ae^{\frac{1}{2}i\Omega T_0} + \bar{A}e^{\frac{-1}{2}i\Omega T_0} + Ne^{i\Omega T_0} + \bar{N}e^{-i\Omega T_0}) - \sigma\,(Ae^{\frac{1}{2}i\Omega T_0} + \bar{A}e^{\frac{-1}{2}i\Omega T_0} + Ne^{i\Omega T_0} + \bar{N}e^{-i\Omega T_0}) + \alpha_2(Ae^{\frac{1}{2}i\Omega T_0} + \bar{A}e^{\frac{-1}{2}i\Omega T_0} + Ne^{i\Omega T_0} + \bar{N}e^{-i\Omega T_0})^2 + g_1 cos(\Omega T_0 + \phi_v)(Ae^{\frac{1}{2}i\Omega T_0} + \bar{A}e^{\frac{-1}{2}i\Omega T_0} + Ne^{i\Omega T_0} + \bar{N}e^{-i\Omega T_0})$$

Rearranging the terms,

$$D_0^2\eta_2 + \frac{1}{4}\Omega^2\eta_2 = e^{\frac{1}{2}i\Omega T_0}[-\sigma A + 2\alpha_2 N\bar{A} - \Omega i(D_1A + \mu A) + \tfrac{1}{2}g_1\bar{A}e^{i\phi_v}] + e^{i\Omega T_0}[-\sigma N + \alpha_2A^2 - 2i\mu\Omega N] + e^{\frac{3}{2}i\Omega T_0}[\tfrac{1}{2}Af_1e^{i\phi v}] + e^{2i\Omega T_0}[\alpha 2N_2 + 12g_1Ne^{i\phi v}] + [\alpha_2(A\bar{A} + N\bar{N}) + 12Ng_1e^{i\phi v}] + \bar{c}. \qquad (18)$$

where $\bar{c}$ is the complex conjugate.

Eliminating the secular terms,

$$-i\Omega D_1A - i\Omega\mu A - \sigma A + \bar{A}\Gamma e^{i\phi_{ee}} = 0 \qquad (19)$$

where

$$\Gamma e^{\phi_{ee}} = 2\alpha_2 N + \frac{1}{2} g_1 e^{i\phi_v} \qquad (20)$$

The solution of equation (18) is of the form,

$$\eta_2 = \frac{-4}{3\Omega^2}[\alpha_2A^2 - (2i\mu\Omega + \sigma)N]e^{iT_0} - \frac{A}{2\Omega^2}\Gamma e^{i(\frac{3}{2}\Omega T_0 + \phi_e e)} + \frac{4}{2}[\alpha_2(A\bar{A} + N\bar{N}) + 12\mathrm{g}_1Ne^{i\phi v}] - \tfrac{4}{15\Omega^2}[\alpha_2N^2 + 12g_1Ne^{i\phi v}]\,\mathrm{e}^{i2\Omega T_0} + \bar{c} \qquad (21)$$

Substituting equations (16) and (21) into (14);

$$D_0^2\eta_3 + \frac{1}{4}\Omega^2\eta_3 = -i\Omega D_2A - D_1^2A - 2\mu D_1A - \frac{-8\alpha_2}{3\Omega^2}[-(2i\mu\Omega + \sigma)N\bar{A} + \alpha_2A^2\bar{A}] - \frac{\alpha_2A\bar{\Lambda}}{\Omega^2}\Gamma e^{i\phi_e e} + \frac{8\alpha_2}{\Omega^2}[2\alpha_2A^2\bar{A} + 2\alpha_2AN\bar{N} + \frac{1}{2}g_1A(\bar{N}e^{i\phi_v} + Ne^{-i\phi_v})] + 6\alpha_3AN\bar{N} + 3\alpha_3A^2\bar{A} - \tfrac{A_1g_1\Gamma}{4\Omega^2}e^{i(\phi_e e - \phi_v)} + g_2A(\bar{N}e^{i\phi_v} + Ne^{-i\phi_v}) + NST + \bar{c} \qquad (22)$$

where NST is the not significant terms and $\bar{c}$ is the complex conjugate.

$$\mathrm{D}_1A = -(\mu + \tfrac{i\sigma}{\Omega})\,\bar{A} + \tfrac{i}{\Omega}\bar{A}\Gamma e^{i\phi_{ee}} \qquad (23)$$

$$\mathrm{D}_1^2A = [\mu^2 - \tfrac{2i\mu\sigma}{\Omega} + \tfrac{\Gamma^2 - \sigma^2}{\Omega^2}]A + \tfrac{2i\mu}{\Omega}\bar{A}\Gamma e^{i\phi_{ee}} \qquad (24)$$

Eliminating the secular terms in equation (22) and then substituting equations (19) and (24);

$$\text{-i}\Omega D_2A + [\mu^2 - \tfrac{\Gamma^2 - \sigma^2}{\Omega^2} - \tfrac{\alpha_2\bar{N}\Gamma}{\Omega^2}\,e^{i\phi_{ee}} + (6\alpha_3 + \tfrac{16\alpha_2^2}{\Omega^2})N\bar{N} + (\bar{N}e^{i\phi_v} + Ne^{-i\phi_v})\,(\tfrac{4\alpha_2f_1}{\Omega^2} + f_2) - \tfrac{\Gamma f_1}{4\Omega^2}e^{i(\phi_{ee} - \phi_v)}]A + (3\alpha_3 + \tfrac{40(\alpha_2)^2}{32})A^2\bar{A} + \tfrac{8_2}{3\Omega^2}(2i\mu\Omega + \sigma)NA = 0 \qquad (25)$$

Using method of reconstitution, the derivative of A with respect to t is found and substituting equation (19) and (25) into equation (9) and equating $\varepsilon = 1$, gives the following,

$$\mathrm{i}\Omega(\dot{A} + \mu_eA) + \sigma_eA - 4\alpha_eA^2\bar{A} - \hat{\Gamma}e^{i\hat{\phi}_e} = 0 \qquad (26)$$

where $\mu_e = \mu - \frac{2\alpha_2q\Gamma}{3\Omega^5}\,sin\,(\phi_{ee} - \phi_e) + \frac{\Gamma g_1}{4\Omega^3}\,sin\,(\phi_{ee} - \phi_v).$ (27)

Also $\sigma_e = \sigma - \mu^2 + \frac{\Gamma^2 - \sigma^2}{\Omega^2} - (\frac{2q}{3\Omega^2})^2\,(6\alpha_3 + \frac{16\alpha_2^2}{\Omega^2}) + \frac{4q}{3\Omega^2}(g_2 + \frac{4\alpha_2g_1}{\Omega^2})cos(\phi_v - \phi_e) - \frac{2q\Gamma\alpha_2}{3\Omega^4}\,cos(\phi_{ee} - \phi_e) + \frac{\Gamma g_1}{4\Omega^2}\,cos\,(\phi_{ee} - \phi_v)$ (28)

where $\alpha_e = \frac{10\alpha_2^2}{3\Omega^2} + \frac{3}{4}\,\alpha_3$ (29)

and

$$\hat{\Gamma}e^{i\hat{\phi}_e} = \Gamma e^{i\phi_{ee}} - \frac{16\alpha_2q}{9\Omega^4}\,(2i\mu\Omega + \sigma)\,e^{i\phi_e}. \qquad (30)$$

Separating the real and imaginary parts gives the equations below,

$$\Omega(\dot{a} + \mu_e a) - a\hat{\Gamma} sin\gamma = 0 \quad (31)$$

$$-\Omega a\dot{\beta} + \sigma_e a - \alpha_e a^3 - a\hat{\Gamma} cos\gamma = 0 \quad (32)$$

where $\gamma = \hat{\phi}_e - 2\beta$. (33)

Therefore

$$\eta = acos[\frac{1}{2}cos(\Omega t + \hat{\phi}_e - \beta)] - \frac{4q}{3\Omega^2}cos(\Omega t + \phi_e) +$$

$$\frac{32\mu q^2}{9\Omega^3}sin(\Omega t + \phi_e) - \frac{16\sigma q}{9\Omega^4}cos(\Omega t + \phi_e) -$$

$$\frac{2a^2\alpha_2}{3\Omega^2}cos(\Omega t + \hat{\phi}_e - \gamma) - \frac{32\alpha_2 q}{135\Omega^6}cos[2(\Omega t + \phi_e)] -$$

$$\frac{ag_1}{4\Omega^2}cos[\frac{3}{2}\Omega t + \phi_v + \frac{1}{2}(\phi_e - \gamma)] + \frac{2\alpha_2}{\Omega^2}(a^2 + \frac{16q^2}{9\Omega^4}) -$$

$$\frac{8g_1 q}{3\Omega^4}cos(\phi_v - \phi_e) + \frac{2\alpha_2 aq}{3\Omega^4}cos[\frac{3}{2}\Omega t + \phi_e + \frac{1}{2}(\hat{\phi}_e - \gamma)] +$$

$$\frac{8g_1 q}{45\Omega^4}cos(2\Omega t + \phi_e + \phi_v) + ... \quad (34)$$

$$\Delta\theta = \theta_{B1}\, cos(\Omega t + \phi_\theta) + acos[\frac{1}{2}(\Omega t + \hat{\phi}_e - \beta)] -$$

$$\frac{4q}{3\Omega^2}cos(\Omega t + \phi_e) + \frac{32\mu q}{9\Omega^3}sin(\Omega t + \phi_e) -$$

$$\frac{16\sigma q}{9\Omega^4}cos(\Omega t + \phi_e) - \frac{2a^2\alpha_2}{3\Omega^2}cos(\Omega t + \hat{\phi}_e - \gamma) +$$

$$\frac{2\alpha_2 aq}{3\Omega^4}cos[\frac{3}{2}\Omega t + \hat{\phi}_e + \frac{1}{2}(\phi_e - \gamma)] -$$

$$\frac{ag_1}{4\Omega^2}cos[\frac{3}{2}\Omega t + \phi_v + \frac{1}{2}(\phi_e - \gamma)] + \frac{2\alpha_2}{\Omega^2}(a^2 + \frac{16q^2}{9\Omega^4}) +$$

$$\frac{8g_1 q}{3\Omega^4}cos(\phi_v - \phi_e) + \frac{32\alpha_2 q^2}{135\Omega^6}cos[2(\Omega t + \phi_e)] +$$

$$\frac{8g_1 q}{45\Omega^4}cos(2\Omega t + \phi_e + \phi_v) + ... \quad (35)$$

Letting $\dot{a} = \dot{\beta} = 0$ in equations (31), (32) and (33),

$$\Omega\mu_e a - \hat{\Gamma} a\, sin\gamma = 0 \quad (36)$$

$$\sigma_e a - \alpha_e a^3 + \hat{\Gamma} a\, cos\gamma = 0 \quad (37)$$

When a=0,

$$\Delta\theta = \theta_{B1}\, cos(\Omega t + \phi_\theta) - \frac{4q}{3\Omega^2}cos(\Omega t + \phi_e) +$$

$$\frac{32\mu q}{9\Omega^3}sin(\Omega t + \phi_e) - \frac{16\sigma q}{9\Omega^4}cos(\Omega t + \phi_e) + \frac{32\alpha_2 q^2}{9\Omega^6} -$$

$$\frac{8g_1 q}{3\Omega^4}cos(\phi_v - \phi_e) + \frac{32\alpha_2 q^2}{135\Omega^6}cos[2(\Omega t + \phi_e)] +$$

$$\frac{8g_1 q}{45\Omega^4}cos(2\Omega t + \phi_e + \phi_v) \quad (38)$$

which is similarly echoed in [6].

When a $\neq 0$, eliminating γ to obtain the frequency response equation,

$$a^2 = \frac{1}{\alpha_e}[\sigma_e \pm \sqrt{(\hat{\Gamma}^2 - \Omega^2\mu_e^2)}] \quad (39)$$

The frequency response plot is obtained with regard to equation (39) which shows the numerical simulation and perturbation solution.

In order to compare the analytical results with the numerical simulations for the case of subharmonic resonance, the following figure, Figure 1, presents phase portraits and time histories when $\Omega = 26.01$ rad/sec.

Using the Runge-Kutta and Newton Raphson methods, the perturbation analysis was simulated and compared to its numerical counterpart. It was determined that the Newton Raphson technique approximates the numerical answer more accurately. The computed numerical error of the Newton Raphson approach and the Runge-Kutta method in comparison to the actual simulation error were 0.0995 and 0.0419, respectively, demonstrating that the Newton Raphson method is a better fit due to the lower error number.

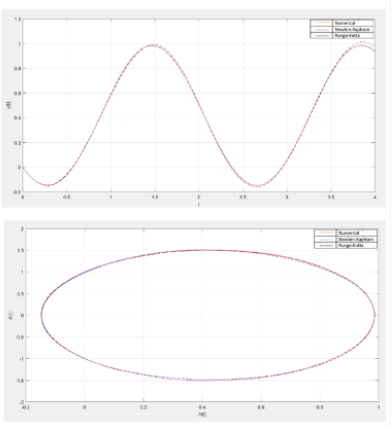

Fig. 1: Perturbed solution employing Runge-Kutta and Newton Raphson algorithms in comparison to numerical simulations for the case of subahrmonic resonance in the phase plane and time history for $\Omega = 26.01$ rad/sec.

Basins of Attractions
(i) Primary Resonance

This resonance plays a vital role in understanding the stability of a nonlinear system. Hence it is important to study the basins of attraction of the primary resonance to obtain more in-depth information about the system. Basins of attraction shows the stable and unstable regions and helps to analyse the changes made to the system, [22]. Plots show the changes in the basins of attraction when variables are altered. It is also necessary to consider boundary conditions when analysing these graphs when arriving at conclusions, [23].

Important insights into the stability behaviour of power systems have been uncovered by studies of the basins of attraction of primary resonance. The effect of parameter variations, including system damping, excitation levels, and control gains, on the shape and magnitude of the basins of attraction associated with primary resonance has been studied, [24], [25]. In addition, research efforts have concentrated on identifying the critical boundaries separating stable and unstable regions in the state space, [26].

(ii) Subharmonic Resonance

The subharmonic resonance analysed in this study further provides evidence on the stable regions of the system. The basins of attractions for the subharmonic resonance depicts the stable and unstable regions when the excitation frequency is approximately double the natural frequency of the dynamical system, [27]. This analysis will show the chaos and instability points of the system for further studies, [28].

Subharmonic resonance's sources of attraction have also been studied extensively. In [29], [30], the authors investigated the effects of various parameters, such as the amplitude and frequency of the subharmonic component, on the basins of attraction. Transitions between distinct subharmonic resonant states and the effect of control strategies on the stability boundaries have been studied, [31], [32]. Hence further investigation on the basins of attraction in necessary to analyse the stability when there is a change in parameters, [33].

2.2 Numerical Analysis
Graphical Representation

The equations (1), (2) and (3) were configured and solved using the fourth-order Runge-Kutta method in Matlab, focusing on the effect of varying the excitation frequency Ω for the subharmonic resonance.

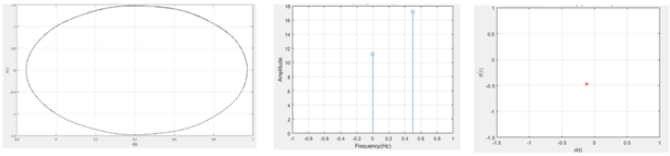

Fig. 2: Phase portrait, frequency-domain plot and Poincaré map when $\Omega = 26.01$ rad/sec.

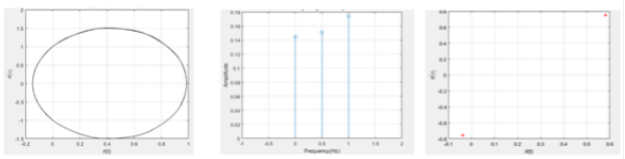

Fig. 3: Phase portrait, frequency-domain plot and Poincaré map when $\Omega = 21.042$ rad/sec.

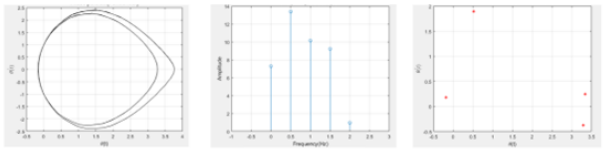

Fig. 4: Phase portrait, frequency-domain plot and Poincaré map when $\Omega = 19.4162$ rad/sec.

Figure 2, Figure 3, Figure 4, Figure 5 and Figure 6 were obtained by plotting the phase portraits, frequency-domain plots, and Poincaré

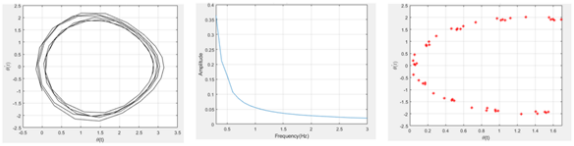

Fig. 5: Phase portrait, frequency-domain plot and Poincaré map when $\Omega = 19.375$ rad/sec.

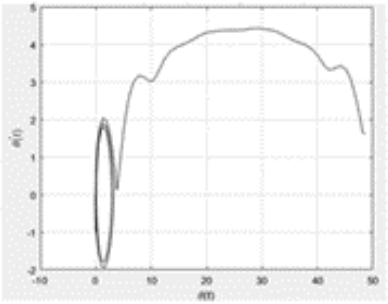

Fig. 6: Phase portrait (loss of synchronism) when $\Omega = 19.37251$ rad/sec.

maps when this excitation frequency is varied in the swing equation (1). As it is decreased the system begins to lose stability and cascades towards chaos. Each plot represents the different period doubling and how the system loses its synchronism. Figure 5 shows that there exists only one steady-state attractor when there is a large Ω, Ω = 26.01 rad/sec. The phase orbit has a closed form and is a period-one attractor. This can be verified using the frequency-domain plot and the Poincaré map.

Furthermore, in Figure 3, the period-one orbit deforms until Ω reaches 21.042 rad/sec, at which point the period-one attractor loses stability and is replaced by a period-two attractor. The frequency-domain plot and Poincaré map show the occurence of the period doubling bifurcation. As Ω is decreased further to 19.4162 rad/sec, the phase portrait illustrates an attractor with two loops.

As the value of Ω is decreased it can be observed that the graphs undergo dynamical transformations including period-doubling solutions and eventually as Ω is decreased to further around $\Omega = 19.375$ rad/sec a chaotic attractor is exhibited as exemplified in Figure 5. The system then loses the synchronism as shown in Figure 6 when the Ω is decreased to the value of 19.37251 rad/sec.

The bifurcation diagram presented as Figure 7, was constructed by solving the swing equation for a specific value of $\Omega = 19.416$ rad/sec and by numerical time integration using the classical fourth order Runge-Kutta algorithm. The forcing r value is incremented slightly and time integration continues plotting the maximum amplitude of the oscillatory solution versus r, [1]:

$$r = \frac{V_G V_B}{X_G} \sin(\theta - \theta_B).$$

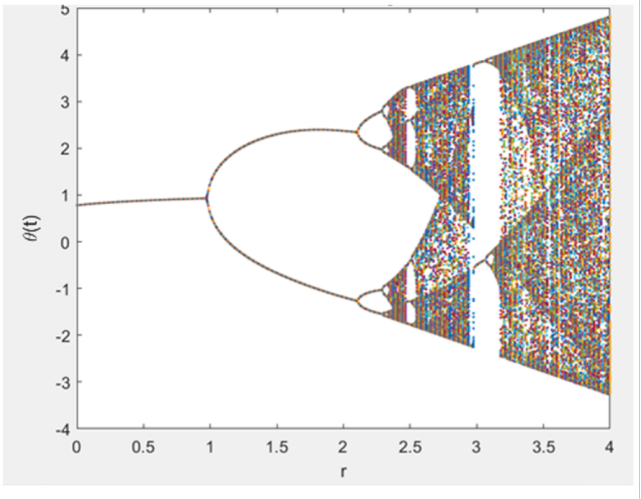

Fig. 7: Bifurcation diagram when r value is varied and constant $\Omega = 19.4162$ rad/sec.

Figure 7 indicates the initial period doubling occurrence just before r = 0.975, also justified by the Poincaré maps of Figure 8 and at around r approximately 2.1, the first period doubling in a sequence of period doubles is exhibited leading to chaotic behaviour.

This numerical analysis shows that the swing equation moves towards loss of synchronisation as the value of r is increased. The corresponding Poincaré maps are plotted as shown, Figure 8. They clearly depict the points where period doubling occurs and how as r is increased the phenomenon of chaos is verified.

Considering the subharmonic resonance, it is observed that at approximately $r > 2.1$, the chaotic region has commenced where the Lyapunov exponent generally takes positive values. This behaviour is depicted and presented as Figure 9, where it is the case when two nearby points, initially separated by an infinitesimal distance, typically diverge from each other over time and this is quantitatively measured by the Lyapunov exponents. The bifurcation diagram of Figure 7, also verifies this behaviour, where at approximately the same value of r, the cascade of period doubling sequence leads to chaos such that

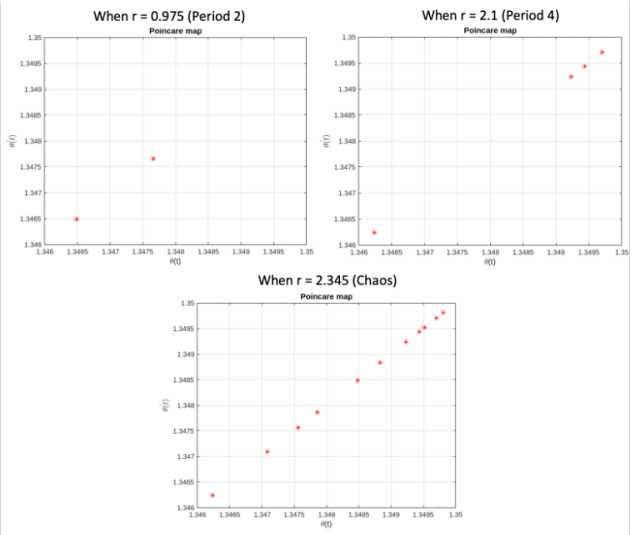

Fig. 8: Poincaré maps for the different r values.

is suffices to say that a chaotic attractor can be identified by a positive Lyapunov exponent. This is further validated through the Poincaré maps shown in Figure 8.

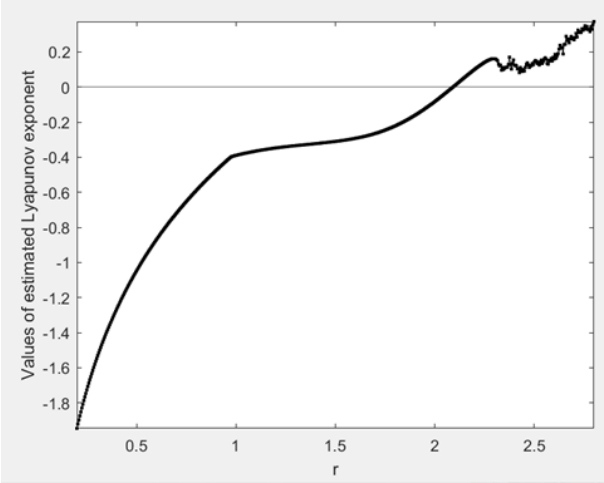

Fig. 9: Lyapunov exponents as r is varied.

To analyse the validity of the analytical solution, it is compared to the numerical simulation and the frequency domain plot for equation (39) is plotted as shown below in Figure 10. This shows a strong concurrence between the two analysis performed on the swing equation for the subharmonic resonance. Hence validating the analysis studied in this paper.

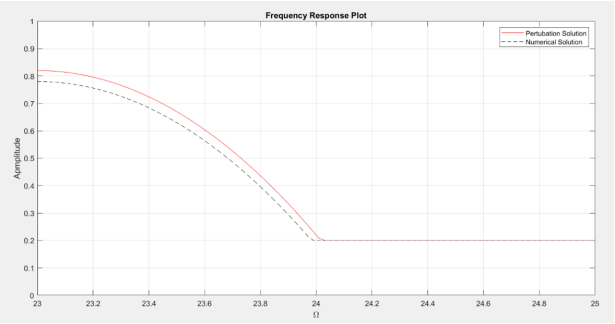

Fig. 10: Frequency domain plot for subharmonic resonance.

(i) Basins of attractions for Primary Resonance

The figures below, Figure 11 and Figure 12, show the basins of attractions for the primary resonance when the variable V_{B1} is varied whilst Ω= 19.375 rad/sec. As the variable is increased the stability of the system changes. The red and green colour show the stable region and the other colours represent the unstable regions of the system. As the variable is increased the system enters a corrupt state with unstable regions, hence a further analysis on the affect of other variables in the system should be considered for sound results in this study.

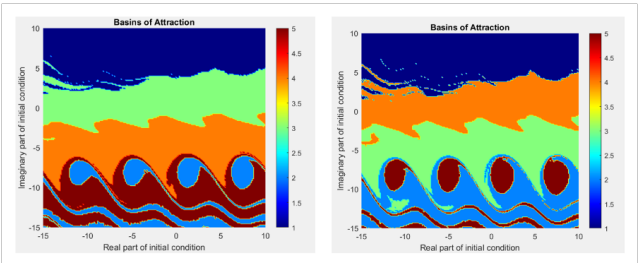

Fig. 11: Basins of attractions when V_{B1} is 0.051 rad and 0.062 rad respectively.

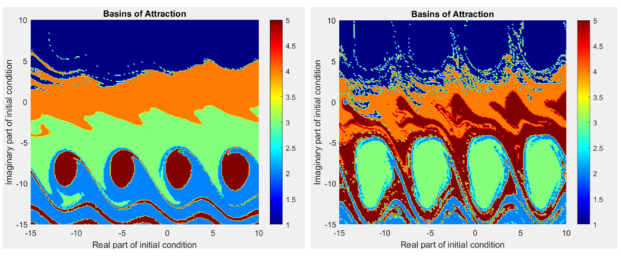

Fig. 12: Basins of attractions when V_{B1} is 0.071 rad and 0.151 rad respectively.

(ii) Basins of attractions for Subharmonic Resonance

Figure 13 and Figure 14 represent the basins of attraction for the subharmonic resonance when V_{B1} and θ_{B1} are varied in the swing equation of the dynamical system. As the variable is changed the system becomes fractal and it becomes corrupt.

Initially only the variable V_{B1} is varied when others are fixed to observe the effect of this particular variable. Even when $V_{B1} = 0$ the system is still corrupted and this is due to the effect of θ_{B1}.

Furthermore, the variable θ_{B1} is changed to observe the transitions in the basins of attractions for subharmonic resonance.

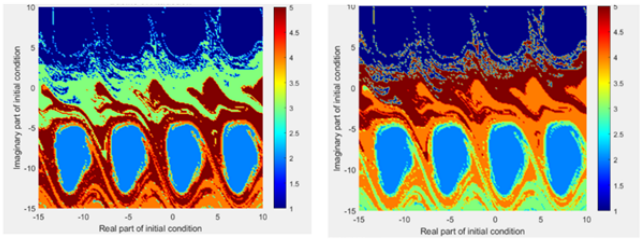

Fig. 13: Basins of attractions when V_{B1} is 0 rad and 0.051 rad respectively.

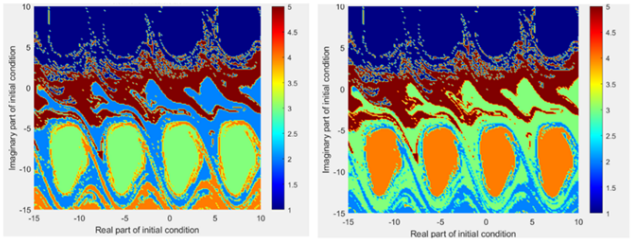

Fig. 14: Basins of attractions when V_{B1} is 0.151 rad and 0.21 rad respectively.

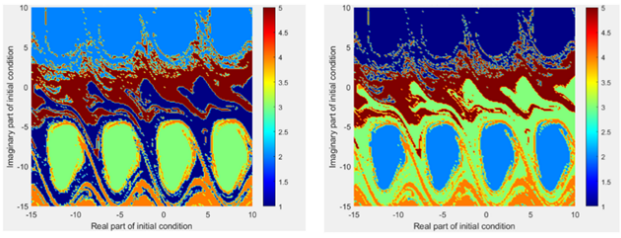

Fig. 15: Basins of attractions when θ_{B1} is 0.191 rad and 0.181 rad respectively.

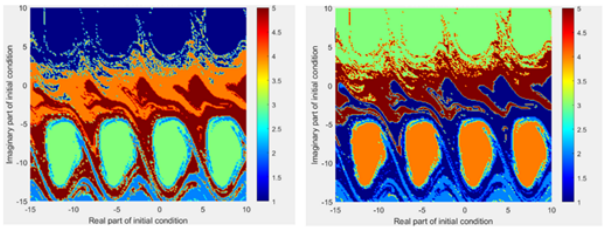

Fig. 16: Basins of attractions when θ_{B1} is 0.151 rad and 0.141 rad respectively.

Figure 15 and Figure 16 depict the system when the variable is varied whilst others are kept constant. In this instance as θ_{B1} is decreased the basins of attractions change and the stable and unstable regions can be observed.

3 Discussion

This paper examines the dynamical behaviour of the swing equation as control parameters are varied. Analytical methods, specifically perturbation techniques, are contrasted with numerical simulation to validate the perturbed solution for subharmonic resonance and the basins of attraction of these phenomena.

The system's behaviour is predicted using the swing equation under a variety of circumstances, such as shifting loads. Power system managers use this data to ensure the stability and dependability of the system. It can be applied to the design and analysis of power system control systems, such as automatic generation control and load frequency management, to minimise blackouts and, more importantly, their potentially catastrophic impacts.

4 Conclusion

In conclusion, the thorough numerical analysis performed in this study, utilising a variety of mathematical tools such as bifurcation diagrams, Lyapunov exponents, phase portraits, frequency domain plots, and Poincaré maps, provided crucial insights into the behaviour of the swing equation under subharmonic resonance. The presence of the first period doubling in a sequence has been identified as a key indicator of impending chaos, signalling potential dangers and operational difficulties for power systems. While period doubling is a well-known scenario for chaotic behaviour, the research has shown that other phenomena, such as intermittency or the collapse of quasi-periodic torus structures, can also result in systemic chaos.

Notably, the study has considered the effects of various parameter variations on the dynamical behaviour of the system, effectively depicting pre-chaotic and post-chaotic changes. The identification of pre-chaos motion patterns provides a clearer comprehension of the transitional behaviour of a system prior to its entry into a chaotic regime. In addition, investigating the basins of attraction for primary and subharmonic resonances has validated the system's loss of stability, which results in chaotic behaviour under subharmonic resonance conditions.

This research contributes considerably to the existing literature on the swing equation, particularly in the power systems domain. By concentrating on primary and subharmonic resonances, this study expands the understanding of the swing equation's fundamental aspects and their implications for system stability. The findings provide valuable direction for power system engineers and researchers, allowing them to develop more effective control strategies and protective measures to mitigate the dangers associated with subharmonic resonance-induced chaos.

This study improves comprehension of the dynamic behaviour of the swing equation and its response to subharmonic resonance, shedding light on the critical factors that determine system stability. As power systems continue to evolve and confront increasingly complex challenges, the findings of this study can help to advance the development of more resilient and secure power infrastructures.

Future research in this area could investigate innovative control methods and technologies to assure the stability and dependability of power systems under subharmonic resonance conditions.

References:

[1] Sofroniou, A., Premnath, B., Munisami, K.J., 2023. An Insight into the Dynamical Behaviour of the Swing Equation 22. https://doi.org/10.37394/23206.2023.22.9

[2] Ji, J. C., and N. Zhang. "Suppression of the primary resonance vibrations of a forced nonlinear system using a dynamic vibration absorber." Journal of Sound and Vibration 329, no. 11 (2010): 2044-2056.

[3] Nayfeh, A.H. and Mook, D.T., 2008. Nonlinear oscillations. John Wiley Sons

[4] Niu, Jiangchuan, Lin Wang, Yongjun Shen, and Wanjie Zhang. "Vibration control of primary and subharmonic simultaneous resonance of nonlinear system with fractional-order Bingham model." International Journal of Non-Linear Mechanics 141 (2022): 103947.

[5] Wang, Xiaodong, Yushu Chen, Gang Han, and Caiqin Song. "Nonlinear dynamic analysis of a single-machine infinite-bus power system." Applied Mathematical Modelling 39, no. 10-11 (2015): 2951-2961.

[6] Nayfeh, Mahir Ali. "Nonlinear dynamics in power systems." PhD diss., Virginia Tech, 1990.

[7] El-Abiad, Ahmed H., and K. Nagappan. "Transient stability regions of multimachine power systems." IEEE Transactions on Power Apparatus and Systems 2 (1966): 169-179.

[8] Sauer, P. W., and M. A. Pai. "Power system steady-state stability and the load-flow Jacobian." IEEE Transactions on power systems 5, no. 4 (1990): 1374-1383.

[9] Qiu, Qi, Rui Ma, Jurgen Kurths, and Meng Zhan. "Swing equation in power systems: Approximate analytical solution and bifurcation curve estimate." Chaos: An Interdisciplinary Journal of Nonlinear Science 30, no. 1 (2020): 013110.

[10] Emam, Samir A., and Ali H. Nayfeh. "On the nonlinear dynamics of a buckled beam subjected to a primary-resonance excitation." Nonlinear Dynamics 35 (2004): 1-17.

[11] Arafat, H. N., and A. H. Nayfeh. "Non-linear responses of suspended cables to primary resonance excitations." Journal of Sound and Vibration 266, no. 2 (2003): 325-354.

[12] Zhao, Chongwen, Zhibo Wang, Jin Du, Jiande Wu, Sheng Zong, and Xiangning He. "Active resonance wireless power transfer system using phase shift control strategy." In 2014 IEEE Applied Power Electronics Conference and Exposition-APEC 2014, pp. 1336-1341. IEEE, 2014.

[13] Kavasseri, Rajesh G. "Analysis of subharmonic oscillations in a ferroresonant circuit." International Journal of Electrical Power Energy Systems 28, no. 3 (2006): 207-214.

[14] KISHIMA, Akira. "Sub-harmonic Oscillations in Three-phase Circuit." Memoirs of the Faculty of Engineering, Kyoto University 30, no. 1 (1968): 26-44.

[15] Deane, Jonathan HB, and David C. Hamill. "Instability, subharmonics and chaos in power electronic systems." In 20th Annual IEEE Power Electronics Specialists Conference, pp. 34-42. IEEE, 1989.

[16] Nayfeh, M. A., A. M. A. Hamdan, and A. H. Nayfeh. "Chaos and instability in a power system—Primary resonant case." Nonlinear Dynamics 1 (1990): 313-339.

[17] Wang, Dong, Junbo Zhang, Wei Cao, Jian Li, and Yu Zheng. "When will you arrive? estimating travel time based on deep neural networks." In Proceedings of the AAAI Conference on Artificial Intelligence, vol. 32, no. 1. 2018.

[18] Zhang, Wei, Fengxia Wang, and Minghui Yao. "Global bifurcations and chaotic dynamics in nonlinear nonplanar oscillations of a parametrically excited cantilever beam." Nonlinear Dynamics 40 (2005): 251-279.

[19] Zulli, D. and Luongo, A., 2016. Control of primary and subharmonic resonances of a Duffing oscillator via non-linear energy sink. International Journal of Non-Linear Mechanics, 80, pp.170-182.

[20] Permoon, M.R., Haddadpour, H. and Javadi, M., 2018. Nonlinear vibration of fractional viscoelastic plate: primary, subharmonic, and superharmonic response. International Journal of Non-Linear Mechanics, 99, pp.154-164.

[21] Kuznetsov, Yuri A., Iu A. Kuznetsov, and Y. Kuznetsov. Elements of applied bifurcation theory. Vol. 112. New York: Springer, 1998.

[22] Alsaleem, F.M., Younis, M.I. and Ouakad, H.M., 2009. On the nonlinear resonances and dynamic pull-in of electrostatically actuated resonators. Journal of Micromechanics and Microengineering, 19(4), p.045013.

[23] Haberman, R. and Ho, E.K., 1995. Boundary of the basin of attraction for weakly damped primary resonance.

[24] Van Cutsem, Thierry, and C. D. Vournas. "Emergency voltage stability controls: An overview." In 2007 IEEE Power Engineering Society General Meeting, pp. 1-10. IEEE, 2007.

[25] Yılmaz, Serpil, and Ferit Acar Savacı. "Basin stability of single machine infinite bus power systems with Levy type load fluctuations." In 2017 10th International Conference on Electrical and Electronics Engineering (ELECO), pp. 125-129. IEEE, 2017.

[26] Parashar, Manu, James S. Thorp, and Charles E. Seyler. "Continuum modeling of electromechanical dynamics in large-scale power systems." IEEE Transactions on Circuits and Systems I: Regular Papers 51, no. 9 (2004): 1848-1858.

[27] Soliman, M.S., 1995. Fractal erosion of basins of attraction in coupled non-linear systems. Journal of sound and vibration, 182(5), pp.729-740.

[28] Nayfeh, M.A., Hamdan, A.M.A. and Nayfeh, A.H., 1991. Chaos and instability in a power system: subharmonic-resonant case. Nonlinear Dynamics, 2, pp.53-72.

[29] Pecora, Louis M., Thomas L. Carroll, Gregg A. Johnson, Douglas J. Mar, and James F. Heagy. "Fundamentals of synchronization in chaotic systems, concepts, and applications." Chaos: An Interdisciplinary Journal of Nonlinear Science 7, no. 4 (1997): 520-543.

[30] Dixit, Shiva, and Manish Dev Shrimali. "Static and dynamic attractive–repulsive interactions in two coupled nonlinear oscillators." Chaos: An Interdisciplinary Journal of Nonlinear Science 30, no. 3 (2020).

[31] Al-Qaisia, A. A., and M. N. Hamdan. "Subharmonic resonance and transition to chaos of nonlinear oscillators with a combined softening and hardening nonlinearities." Journal of sound and vibration 305, no. 4-5 (2007): 772-782.

[32] Butikov, Eugene I. "Subharmonic resonances of the parametrically driven pendulum." Journal of Physics A: Mathematical and General 35, no. 30 (2002): 6209.

[33] Nusse, Helena E., and James A. Yorke. Dynamics: numerical explorations: accompanying computer program dynamics. Vol. 101. Springer, 2012.

Contribution of individual authors to the creation of a scientific article (ghostwriting policy)

All authors contributed to the development of this paper. Conceptualisation, Anastasia Sofroniou; Methodology, Anastasia Sofroniou and Bhairavi Premnath; Analytical and Numerical Analysis Bhairavi Premnath; Validation, Anastasia Sofroniou and Bhairavi Premnath; Writing-original draft preparation, Bhairavi Premnath and Anastasia Sofroniou; Writing-review and editing, Anastasia Sofroniou and Bhairavi Premnath; Supervisor, Anastasia Sofroniou.

Sources of Funding for Research Presented in a Scientific Article or Scientific Article Itself

No funding was received for conducting this study.

Conflict of Interest

The authors have no conflicts of interest to declare that are relevant to the content of this article.